Supplemental Materials

Microcystin-RR is a biliary toxin selective for neonatal cholangiocytes

Kapish Gupta[1,2], Dongning Chen[1,2,3], Rebecca G. Wells[1,2,3] *

[1]Division of Gastroenterology and Hepatology, Department of Medicine, University of Pennsylvania, Philadelphia, PA, USA

[2]Center for Engineering MechanoBiology, University of Pennsylvania, Philadelphia, PA, USA

[3]Department of Bioengineering, University of Pennsylvania, Philadelphia, PA, USA

Corresponding author: Rebecca G. Wells

Supporting Material and Methods

Treatment of cholangiocyte monolayers

Cholangiocytes were cultured on collagen-coated dishes and treated with various concentrations of microcystins dissolved in 0% BEC media. Cell viability was assessed using the MTT assay, and apoptosis was measured using TUNEL staining. Additionally, microcystin retention was evaluated by treating cells with 400 nM MC-RR and MC-LR for 24 h, followed by washing with 1X PBS three times and incubation with 1X RIPA buffer for 30 min. The amount of microcystin in the cell lysate was then quantified using a Microcystin (Adda specific) ELISA kit, following the manufacturer's instructions (Prod. No. ALX-850-319, Enzo Life Science Inc. Farmingdale, NY, United States).

Treatment of spheroids

Cholangiocytes were plated in a collagen-Matrigel mixture [1] and allowed to form spheroids for 6-8 days. These spheroids were then treated with 400 nM individual microcystins, 400 nM nodularin, or vehicle in 0% BEC media. To perform washout experiments, spheroids were treated with 400 nM MC-RR or vehicle control in 0% BEC media for 15 or 24 h, washed three times with 1X PBS, and then placed in 0% BEC media for 9 or 24 h, respectively. For rescue experiments, spheroids were treated with 400 nM MC-LR or MC-RR and drugs (20 μM NAC, 500 nM suramin, or 2 μM pranlukast [2] obtained from Invitrogen, Waltham, MA, USA) in 0% BEC media for 24 h. Subsequently, spheroids were fixed, stained, and imaged using a confocal microscope to evaluate spheroid morphology.

EHBD explant treatment

EHBD explants were treated with individual microcystins or vehicle in 0% BEC media in a Vitron Dynamic Organ Culture Incubator (San Jose, United States) for 24 h as described in [3]. For rescue experiments, EHBD were treated for 24 h with 400 nM MC-RR or 400nM MC-RR and 20 μM NAC in 0% BEC media. Following treatment, all EHBDs were stained as described below.

Immunofluorescence staining.

Spheroids and EHBDs were fixed with paraformaldehyde, permeabilized using 0.5% Triton X-100 in PBS, and subsequently blocked with a blocking solution containing 10% FBS and 0.1% Triton X-100 in PBS. Immunostaining was performed as described previously (3) using antibodies listed in Table S1.

Quantitative real-time PCR

EHBDs from P2 (6 ducts per sample) and adult (3 ducts per sample) mice were homogenized using a Bullet Blender® Homogenizer and RNA was isolated using TRIzol™ Reagent (Invitrogen) according to the manufacturer's instructions. 3 pooled samples each for P2 and adults were used. RNA concentrations were measured with a NanoDrop ND-1000 full-spectrum spectrophotometer (ThermoFisher Scientific, Wilmington, MA, USA). Single-stranded complementary DNA (cDNA) was synthesized using the SuperScript VILO cDNA Synthesis Kit (ThermoFisher) according to the manufacturer's instructions. cDNA was diluted to 2 ng/µL for real-time quantitative PCR analysis and PCR reactions were performed using Taqman Mastermix (Applied Biosystems, ThermoFisher Scientific, Waltham, MA, USA) in a total volume of 10 µL. Real-time quantitative PCR was done for genes involved in oxidative response and for Organic anion transport protein (OATP) genes (also known as solute carrier organic anion transporters or Slco). The following predesigned primers were purchased from ThermoFisher: Sod (Mm01344233_g1), Gpx-1 (Mm00656767_g1), Cat (Mm00437992_m1), Gpx-4 (Mm04411498_m1), Gsto-1(Mm00599866_m1), Slco1a1 (Mm01267415_m1), Slco1a6 (Mm01267368_m1), Slco2a1 (Mm00459638_m1), Slco1a4 (Mm01267407_m1), Slco1b2 (Mm00451510_m1) and Slco2b1 (Mm00614448_m1). Thermal cycling and fluorescence detection were performed on a StepOnePlus Real-Time PCR system from ThermoFisher. Expression levels were corrected using a reference gene (ΔCt). For OATP genes, only 2a1 and 2b1 showed detectable expression ($2^{-\Delta Ct}$) in both P2 and adult samples. All the genes involved in oxidative responses showed detectable expression. All PCR results results are shown as expression relative to expression in adults ($2^{-\Delta Ct\_Sample}/2^{-\Delta Ct\_Adults}$).

Glutathione (GSH) measurements

EHBD from P2 (4 ducts per sample) and adult (2 duct per sample) mice were homogenized using a Bullet Blender® Homogenizer in the presence of RIPA buffer (Invitrogen) and protease inhibitors. 6 pooled samples each for P2 and adults were used. Samples were centrifuges to remove debris. GSH was determined using Mouse GSH ELISA Kit (MyBioSource, Inc. San Diego, CA, USA) and protein content was determined using a micro BCA protein assay reagent kit (ThermoFisher Scientific). GSH per mg protein was determined for each sample. The results are shown as expression relative to expression in adults ($GSH_{Sample}/GSH_{|Adult|}$).

ROS measurements

Spheroids were treated with DMSO, 400 nM MC-LR, or 400 nM MC-RR for 24 h. After washing in 1X PBS, the spheroids were incubated with 5 µM CellRox Green for 30 min at 37°C. The samples were washed and counterstained with phalloidin and DAPI according to the manufacturer's instructions, and then imaged.

References:

[1] Waisbourd-Zinman O, Koh H, Tsai S, Lavrut P-M, Dang C, Zhao X, et al. The toxin biliatresone causes mouse extrahepatic cholangiocyte damage and fibrosis through decreased glutathione and SOX17. Hepatology 2016;64:880–93. https://doi.org/10.1002/hep.28599.

[2] Kamo S, Nakanishi T, Aotani R, Nakamura Y, Gose T, Tamai I. Impact of FDA-Approved Drugs on the Prostaglandin Transporter OATP2A1/SLCO2A1. J Pharm Sci 2017;106:2483–90. https://doi.org/10.1016/j.xphs.2017.04.046.

[3] Chen Y, Gilbert MA, Grochowski CM, McEldrew D, Llewellyn J, Waisbourd-Zinman O, et al. A genome-wide association study identifies a susceptibility locus for biliary atresia on 2p16.1 within the gene EFEMP1. PLoS Genet 2018;14:e1007532. https://doi.org/10.1371/journal.pgen.1007532.

Supporting Table S1: List of antibodies and stains

Primary Antibodies				
Antigen	**Host**	**Supplier**	**Cat. No.**	**Dilution**
KRT19	Rabbit	Abcam, Boston, MA, USA	ab52625	1:100
Vimentin	Chicken	Novus Biologicals, Centennial, CO USA	NB300-223	1:100
Ki67	Rabbit	Abcam	Ab16667	1:100
ZO-1	Rabbit	Invitrogen	61-7300	1:50
Secondary Antibodies				
Antigen	**Host**	**Supplier**	**Cat. No.**	**Dilution**
Rabbit	Donkey	Jackson ImmunoResearch Laboratories, Inc, West Grove, PA, USA	711-165-152	1:300
Chicken	Donkey	Jackson ImmunoResearch Laboratories, Inc	703-605-155	1:300
Stains				
Dye	**Target**	**Supplier**	**Cat. No.**	**Concentration**
DAPI	Nucleus	Invitrogen	D1306	1 µg/mL
Rhodamine Phalloidin	Actin	Invitrogen	R415	0.33 µM
CellRox Green	ROS	Invitrogen	C10444	5 µM

List of Supporting Figures

Supporting Figure S1: **Quantification of lumen closure in EHBD cholangiocyte spheroids.** A) Z-stacks (step size 5 μm) were obtained using confocal microscopy. Image shows all the slices for a representative spheroid. B) To quantify lumen closure, a Z-projection image was created and used to create a spheroid mask. The mask was eroded by 1 cell thickness (calculated by taking the average of the shortest diameter or width of 3 cells) to obtain theoretical lumen (TL) area, assuming a cell layer one cell thick. To calculate the actual lumen (AL) area, the middle Z-stack was used to create a mask. The relative difference in theoretical and actual lumen area was used to calculate "% lumen closure". Red: actin, Blue: DAPI. All scale bars 50 μm.

Supporting Figure S2: **Imaging and representation of EHBD**: A) Explant culture of EHBD in high oxygen incubator, without treatment. EHBDs were stained and imaged with confocal microscopy. Images were captured at 5 μm intervals relative to the "base" image, where the monolayer was visible. The images are displayed with respect to this base image, and each z-slice was annotated based on its distance from the base. The EHBD schematic depicts two sections: one at the base and another at X μm distance from the base. B) Representative image showing all the z-slices obtained for one EHBD. In Figure 4 only the "base" and "base+20 μm" slices are shown. C) 3-D rendering of the EHBD shown in B. Red: KRT19, Blue: DAPI. Scale bar 50 μm.

Supporting Figure S3: **EHBD damage quantification.** EHBDs were placed in one of three groups depending on the degree of damage, as assessed after KRT19 staining (red). A) EHBDs that showed cholangiocytes with a cobblestone morphology (white arrow) and forming a continuous monolayer (orange arrowhead) surrounding the lumen (L) were considered "normal". B) EHBDs with abnormally-shaped cholangiocytes (white arrow) and disrupted monolayers (orange arrowhead) but with open lumens (L) were placed in the "partial damage" group. C) EHBDs with misshapen cholangiocytes (white arrow), a disrupted monolayer (orange arrowhead), and a closed lumen (L) were placed in the "complete damage" group. Red: KRT19. Scale bar 50 μm.

Supporting Figure S4: **Neonatal EHBD cholangiocytes form hollow spheroids with apical/basal polarity.** A) A control (untreated) spheroid stained with actin and KRT19. B-D) Intensity scans across lines marked as B, C and D in merged panel in A. Basal (BL) and apical (AP) regions are marked with purple and green rectangles. The cells have preferential apical actin localization and express more KRT19 apically. Nuclei are central. Ratio of maximum actin intensity in apical and basal sections, as determined by this method, was used in the quantification for main Fig. 2C. E) Representative image showing a cross-section of cholangiocytes cultured in a collagen-Matrigel mixture for 6 d and treated with vehicle for 24 h. Cells arrange themselves into hollow spheroids as shown in the 3D reconstruction. Red: actin, Green: KRT19, Blue: DAPI; all scale bars 50 μm.

Supporting Figure S5: **Washout after MC-RR treatment does not rescue MC-RR-induced damage**. Representative images (similar to those in main Fig. 3) showing spheroids treated with 400 nM MC-RR for 15 and 24 h, with washout for 9 and 24 h, respectively. In both cases, removal of MC-RR with washout was not sufficient for rescue. Quantification in main Fig. 3. Red: actin, Blue: DAPI. All scale bars 50 μm.

Supporting Figure S6: **MC-RR-induced damage to neonatal rat EHBD explants**. A) 3D reconstruction of representative EHBD isolated from P2 rat and cultured as explant in a high oxygen incubator. B) 3D reconstruction of representative EHBD isolated from P2 rat cultured similarly but in the presence of 400 nM MC-RR for 24 h. Red: KRT19.

Supporting Figure S7: **Mechanism of MC-RR-induced damage in neonatal mouse EHBD cholangiocyte spheroids.** A) Representative image of control spheroids (treated with vehicle) and stained for Ki67 and vimentin. B) Representative image showing MC-RR-treated spheroids stained for Ki67 and vimentin. C) Quantification of vimentin staining intensity in EHBD cholangiocyte spheroids after treatment with 400 nM MC-RR for 24 h with a minimum of 18 spheroids for each condition quantified. D) TUNEL positive cells were measured after treatment with vehicle or 400 nM MC-RR for 24 h. Quantification from three independent experiments. E) MTT assay after treatment of cholangiocytes with MC-RR at concentrations up to 1.6 mM. Quantification from three independent experiments. Cyan: vimentin, Red: actin, Green: Ki67, Blue: DAPI. All scale bars 50 μm.

Supporting Figure S8: **Vimentin expression in EHBDs treated with MC-RR and NAC**. Representative images showing expression of vimentin in damaged cholangiocytes in EHBD explants in the presence of vehicle (control), 300 nM MC-RR, 400 nM MC-RR and 300 nM MC-RR+20 μM NAC for 24 h. White arrowheads highlight cells co-stained with KRT19 and vimentin. The last panel of each row shows the magnification of the yellow inset in the merged image. Cyan: vimentin, Red: KRT19, Blue: DAPI. All scale bars 50 μm.

Supporting Figure S9: **OATP inhibition does not rescue MC-RR-induced damage**. A) Relative mRNA expression of OATP 2a1 and 2b1 in neonatal EHBD compared to adult EHBD. OATP 1a1, 1a4, 1a6 and 1b2 were below the detection limit in neonatal samples (n=3). B) Quantification showing no difference in MC-RR-induced lumen damage following OATP 2a1 inhibition using suramin and pranlukast (n=18 spheroids per condition from 3 independent experiments). C) Representative images showing neonatal spheroid damage in the presence of 400 nM MC-RR and 500 nM suramin for 24 h. D) Representative images showing neonatal spheroid damage in presence of 400 nM MC-RR and 2 μm pranlukast for 24 h. Red: actin, Blue: DAPI. All scale bars 50 μm.

Supporting Figure S10: **MC-RR specifically induces ROS in neonatal EHBD cholangiocyte spheroids**. Representative images showing spheroids from adult and neonatal EHBD cholangiocytes treated with vehicle, 400 nM MC-LR and 400 nM MC-RR for 24 h. ROS were observed only in neonatal EHBD cholangiocytes treated with 400 nM MC-RR. Quantification in main Figure 6E. Red: actin, Green: Cell Rox Green, Blue: DAPI. All scale bars 50 μm.

Supporting Figure S11: **Neonates have immature antioxidant defense systems**. A) GSH levels were quantified in protein samples obtained from P2 and adult mice, showing significantly lower GSH levels in neonates compared to adults (n=6). B) RNA samples from P2 and adult mice were analyzed for enzymes involved in antioxidant defense systems, demonstrating that all measured enzymes except GSTO-1 were significantly lower in neonates compared to adults (n=3).

Supporting Figure S12: **NAC rescues cholangiocyte damage in cholangiocytes treated with 300 nM MC-RR**. Representative images showing spheroids treated with 300

and 400 nM MC-RR with and without 20 μM NAC for 24 h. Red: actin, Blue: DAPI. All scale bars 50 μm.

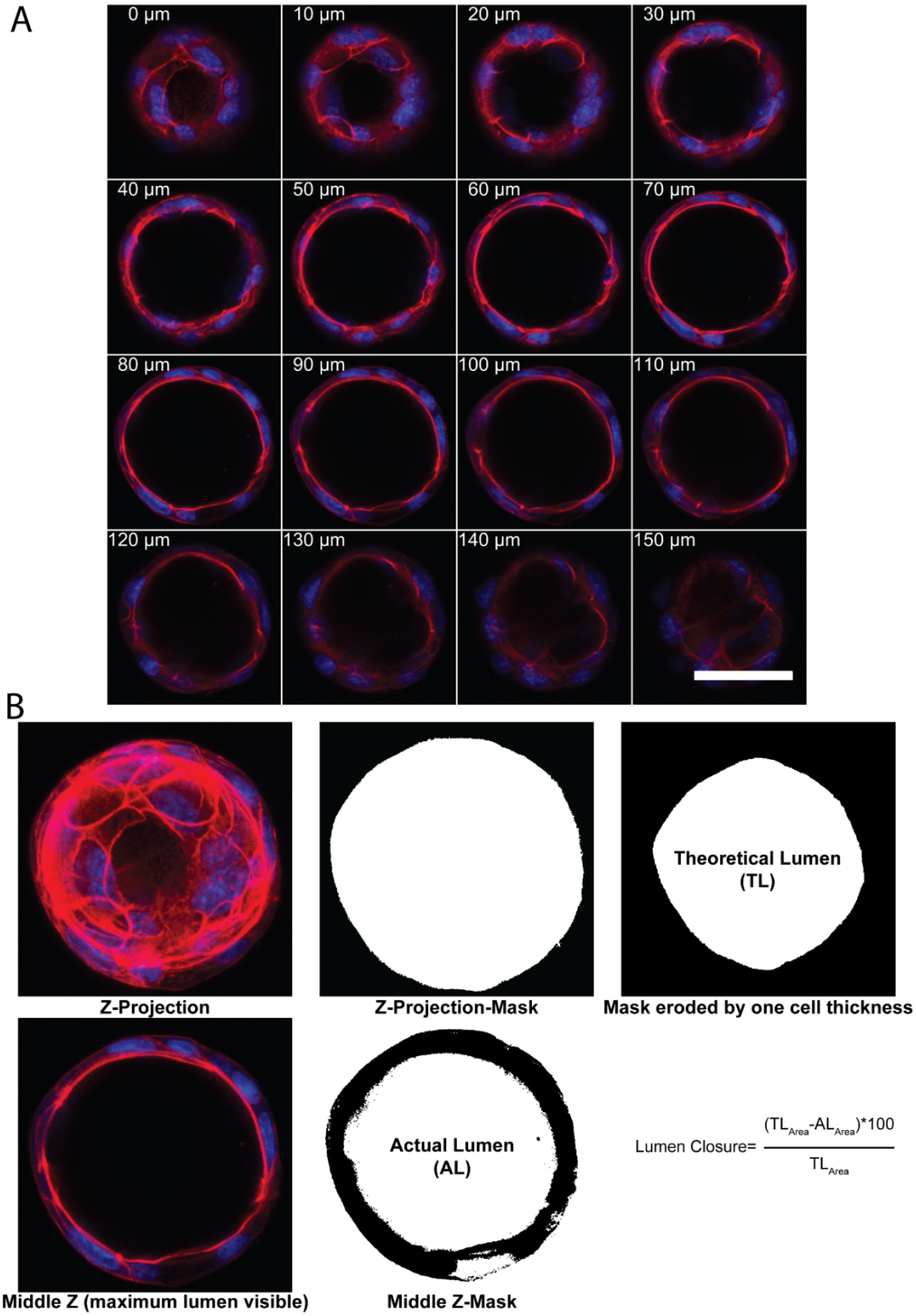

Supporting figure S1

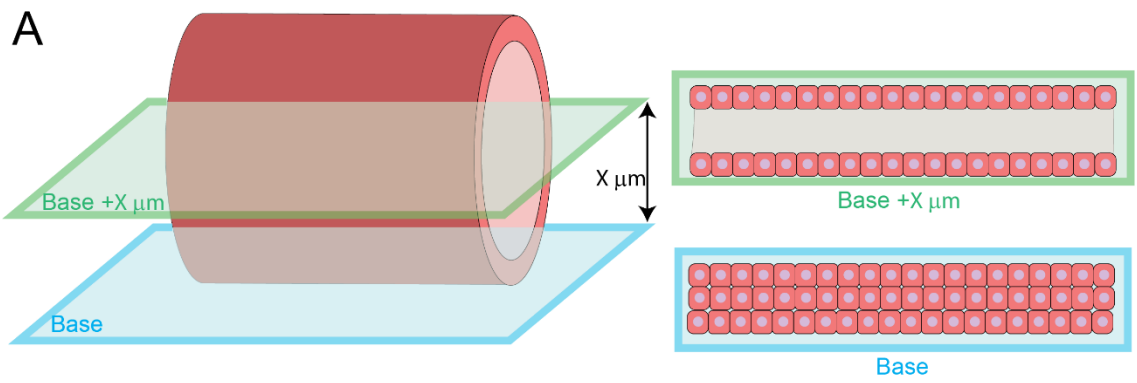

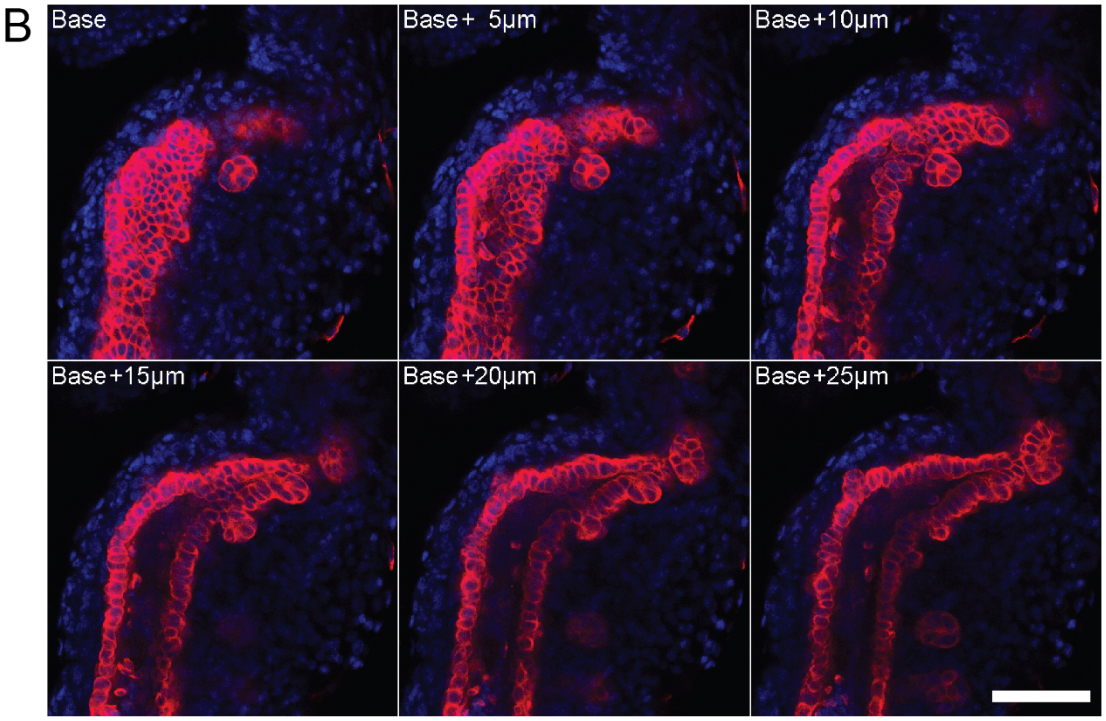

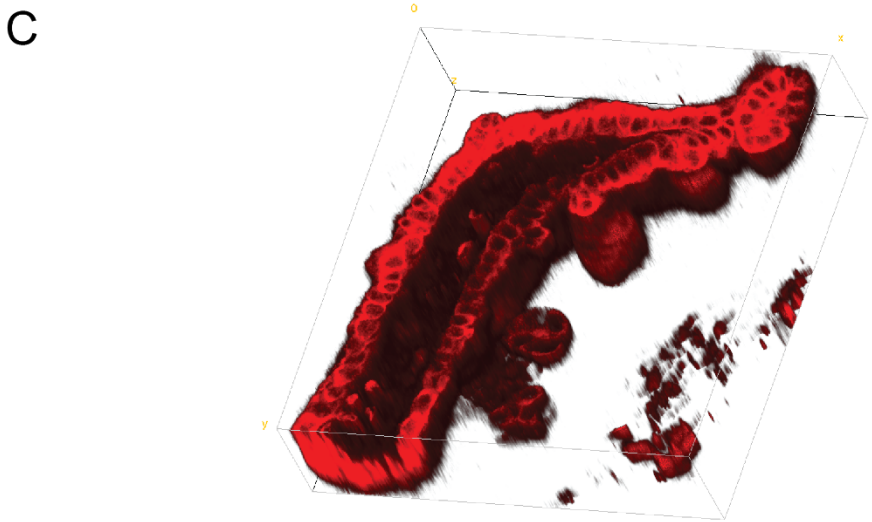

Supporting figure S2

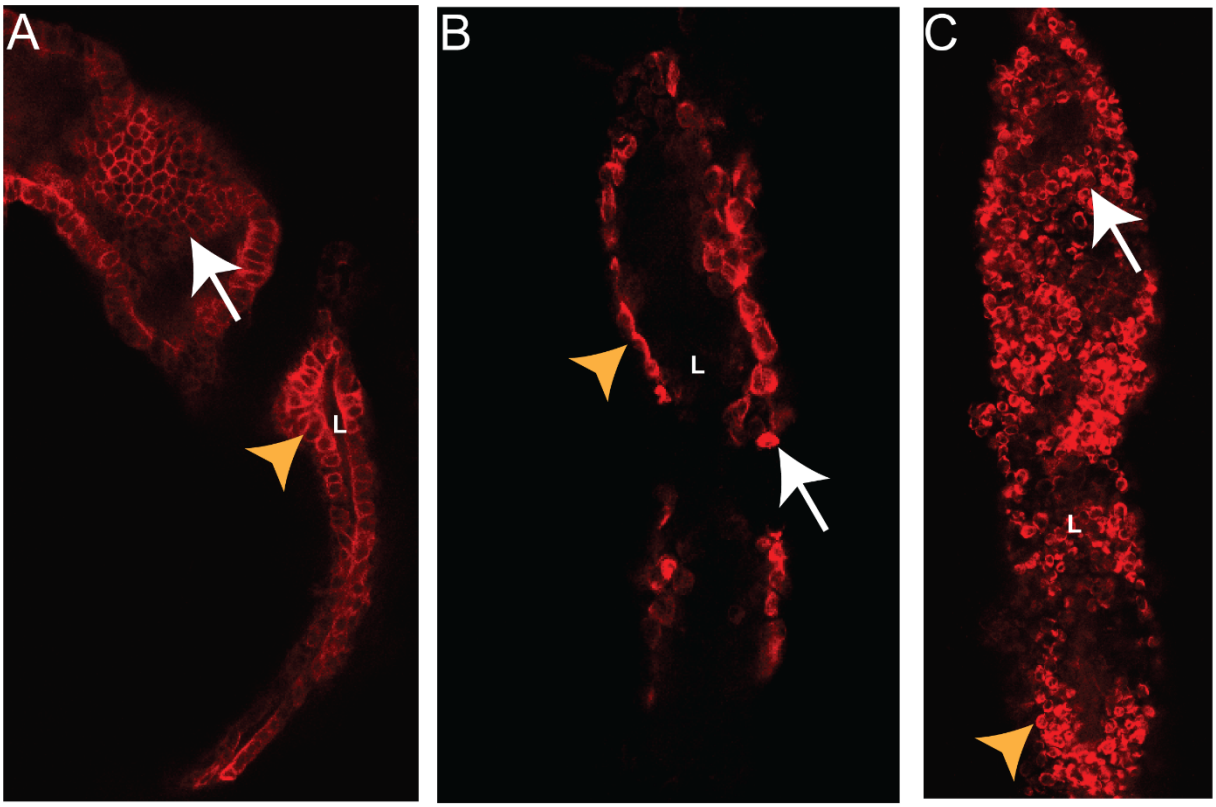

Normal	**Partial Damage**	**Complete Damage**
1. Cobblestone-shaped cholangiocytes (white arrow)	1. Cobblestone-shape disrupted in cholangiocytes (white arrow)	1. Cobblestone-shape disrupted in cholangiocytes (white arrow)
2. Monolayer integrity maintained (yellow arrowhead)	2. Monolayer partially disrupted (yellow arrowhead)	2. Monolayer integrity disrupted (yellow arrowhead)
3. Lumen seen (L)	3. Lumen seen (L)	3. Lumen filled (L)

Supporting figure S3

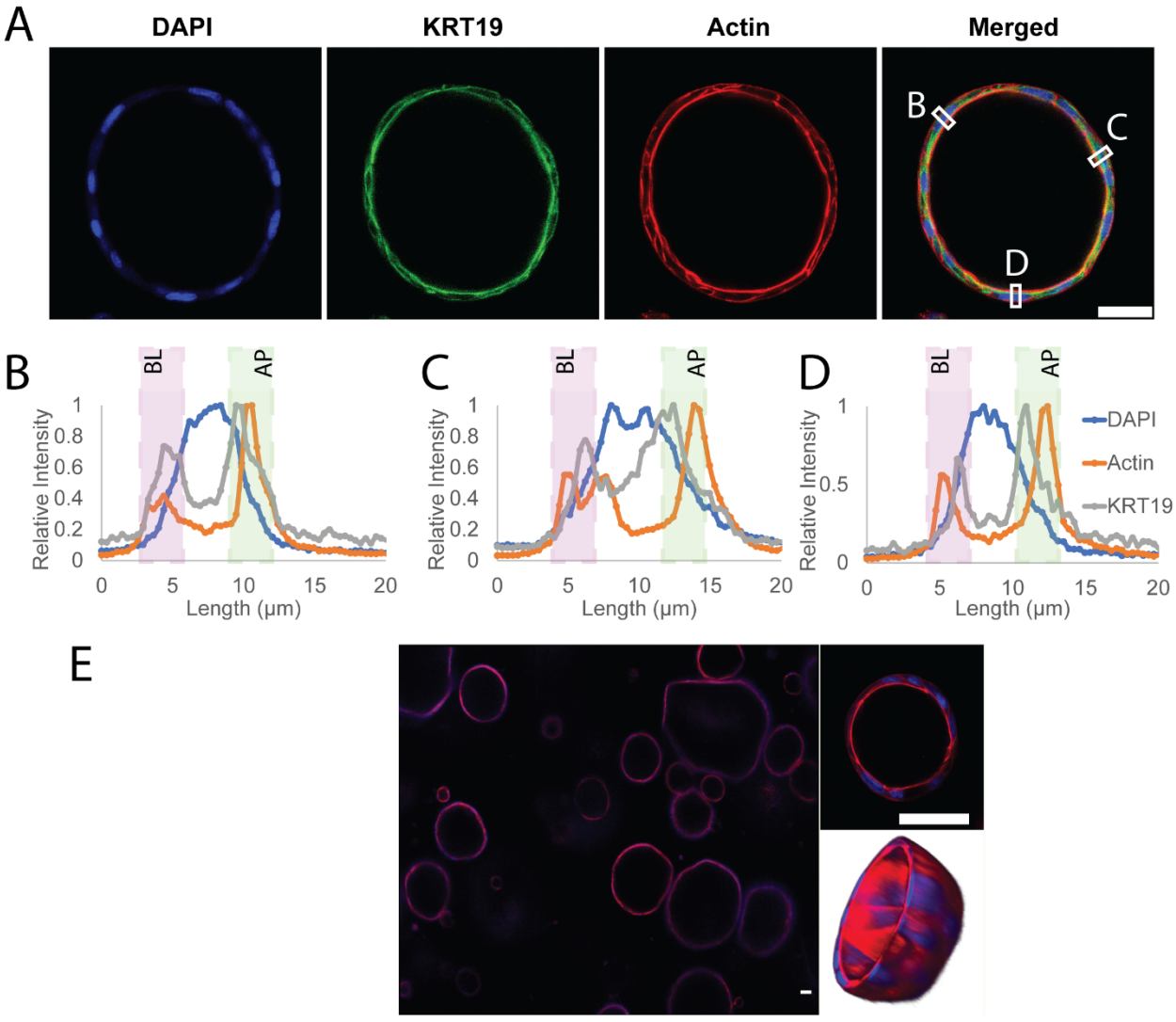

Supporting figure S4

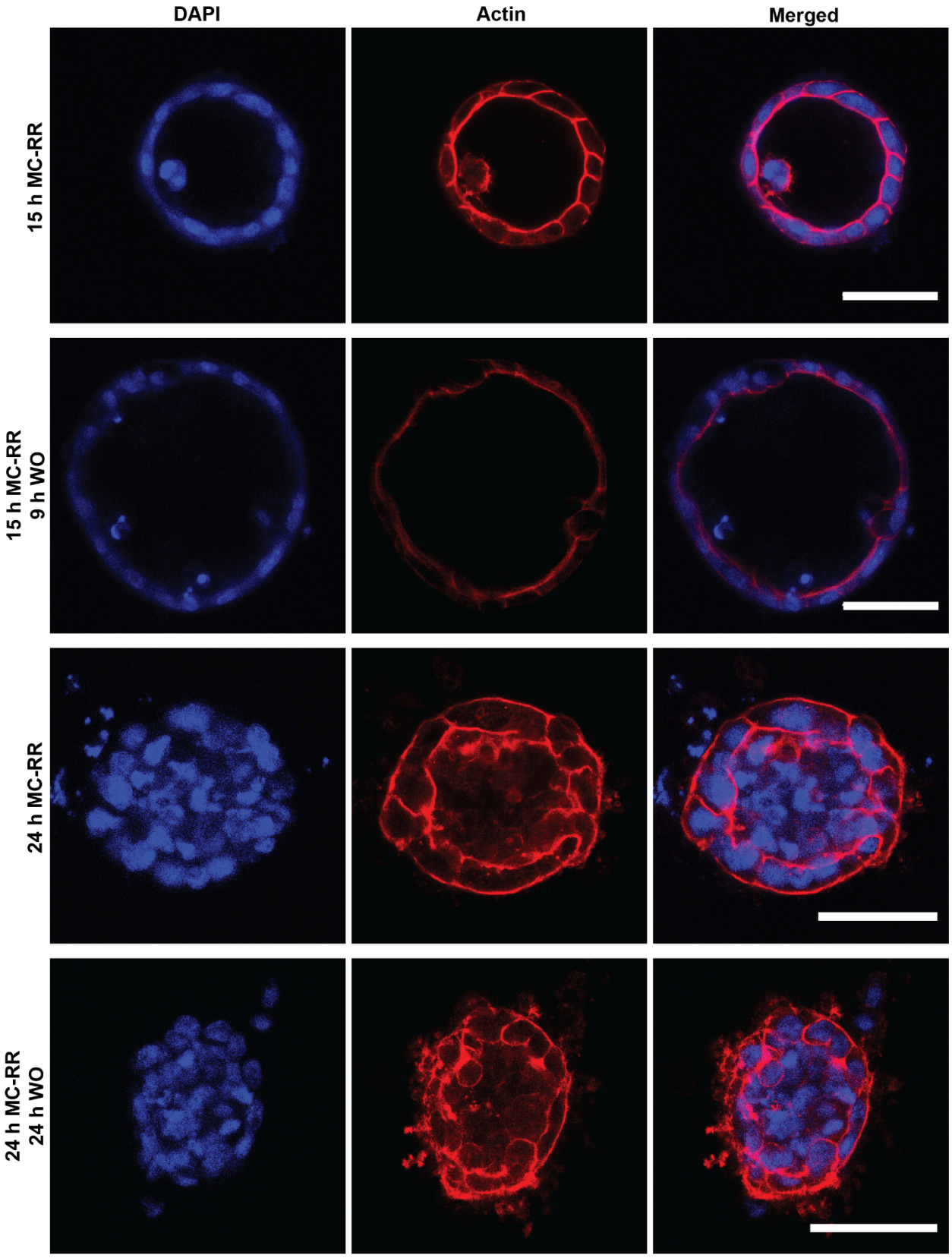

Supporting figure S5

A

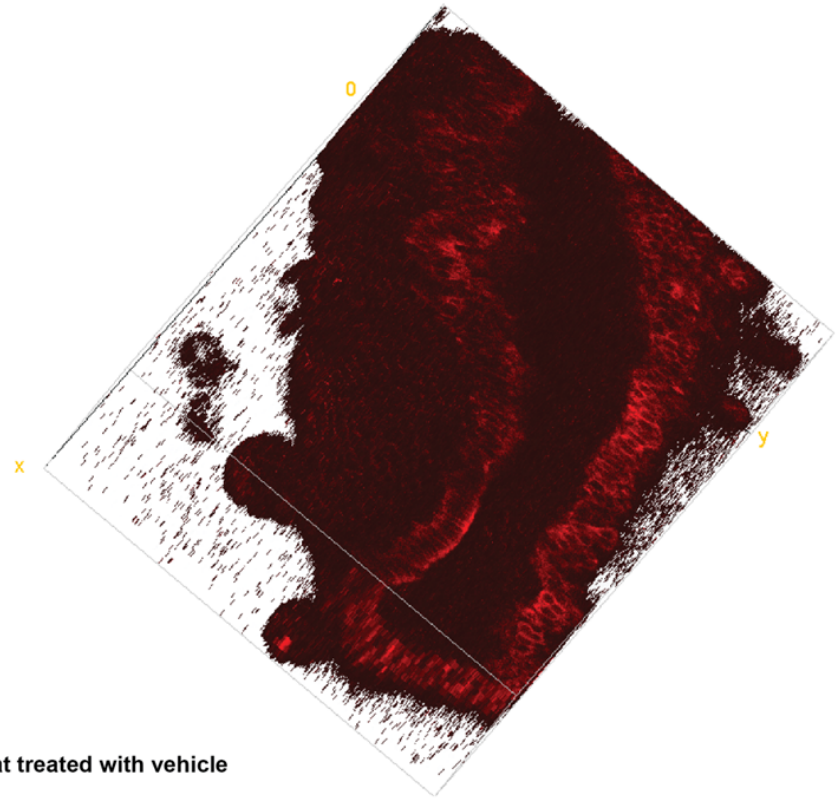

2-day old rat treated with vehicle

B

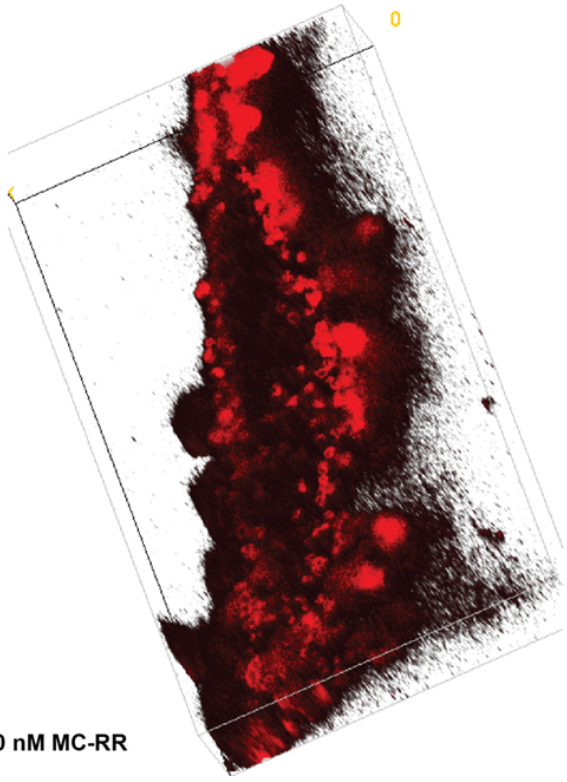

2-day old rat treated with 400 nM MC-RR

Supporting figure S6

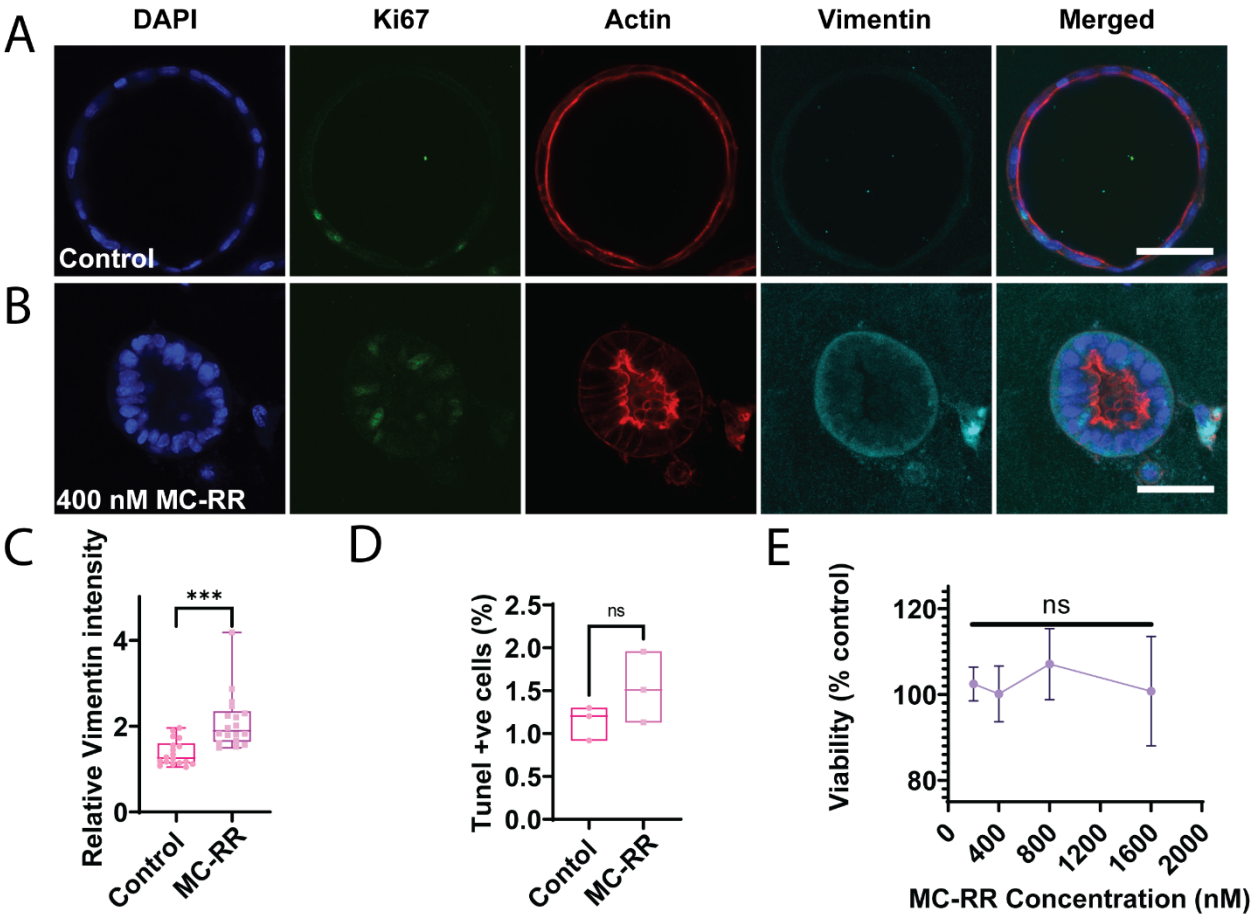

Supporting figure S7

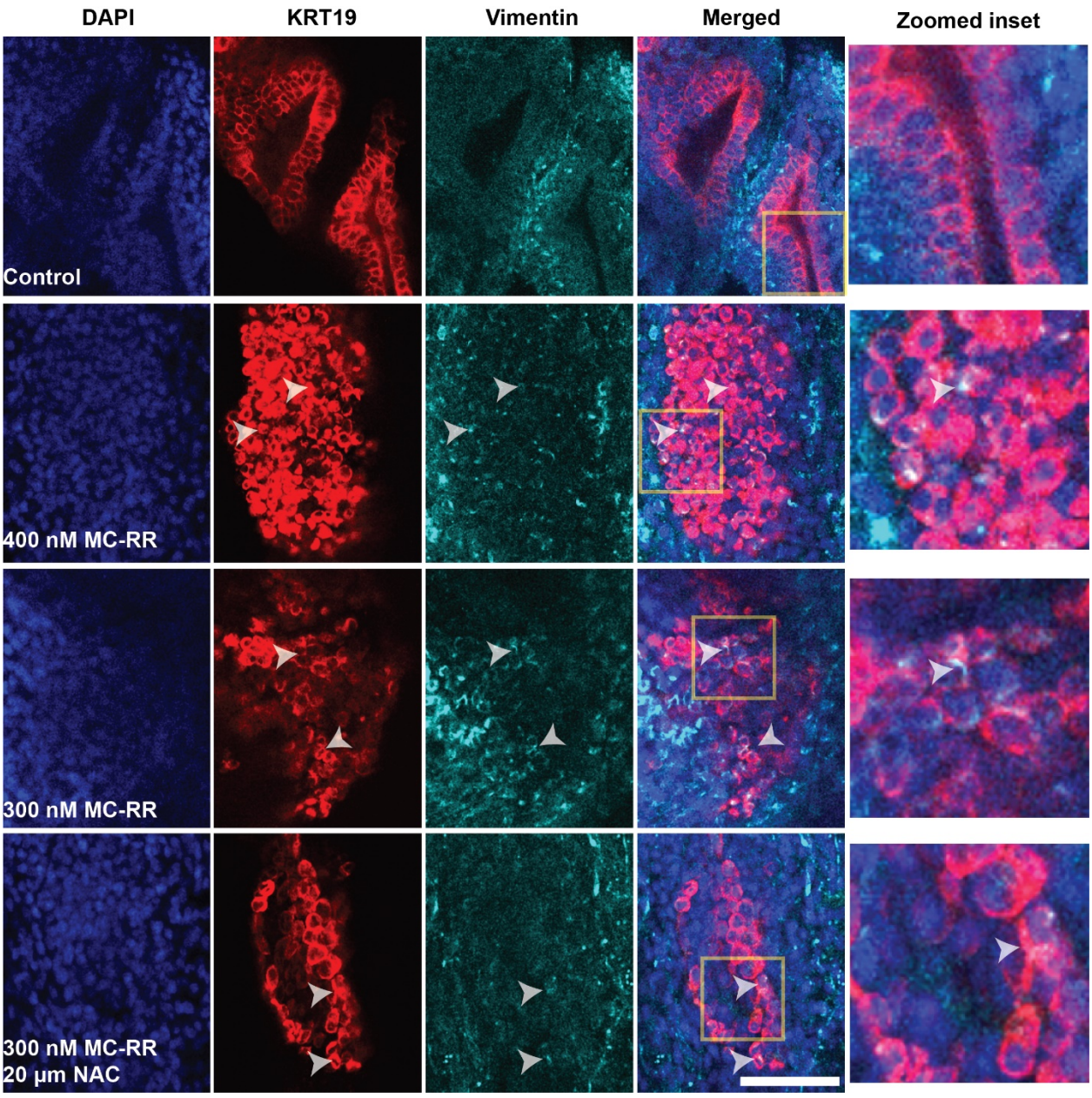

Supporting figure S8

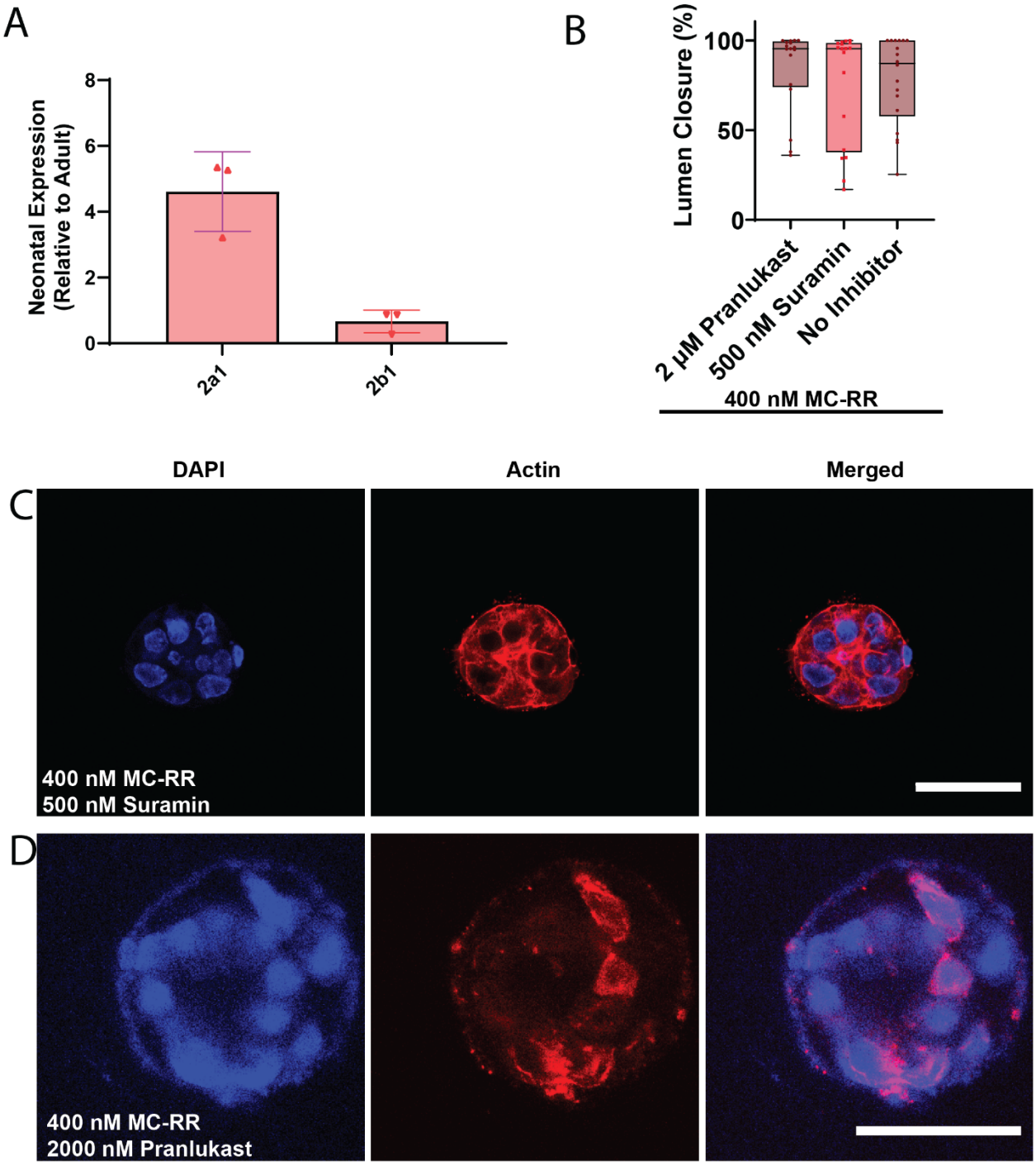

Supporting figure S9

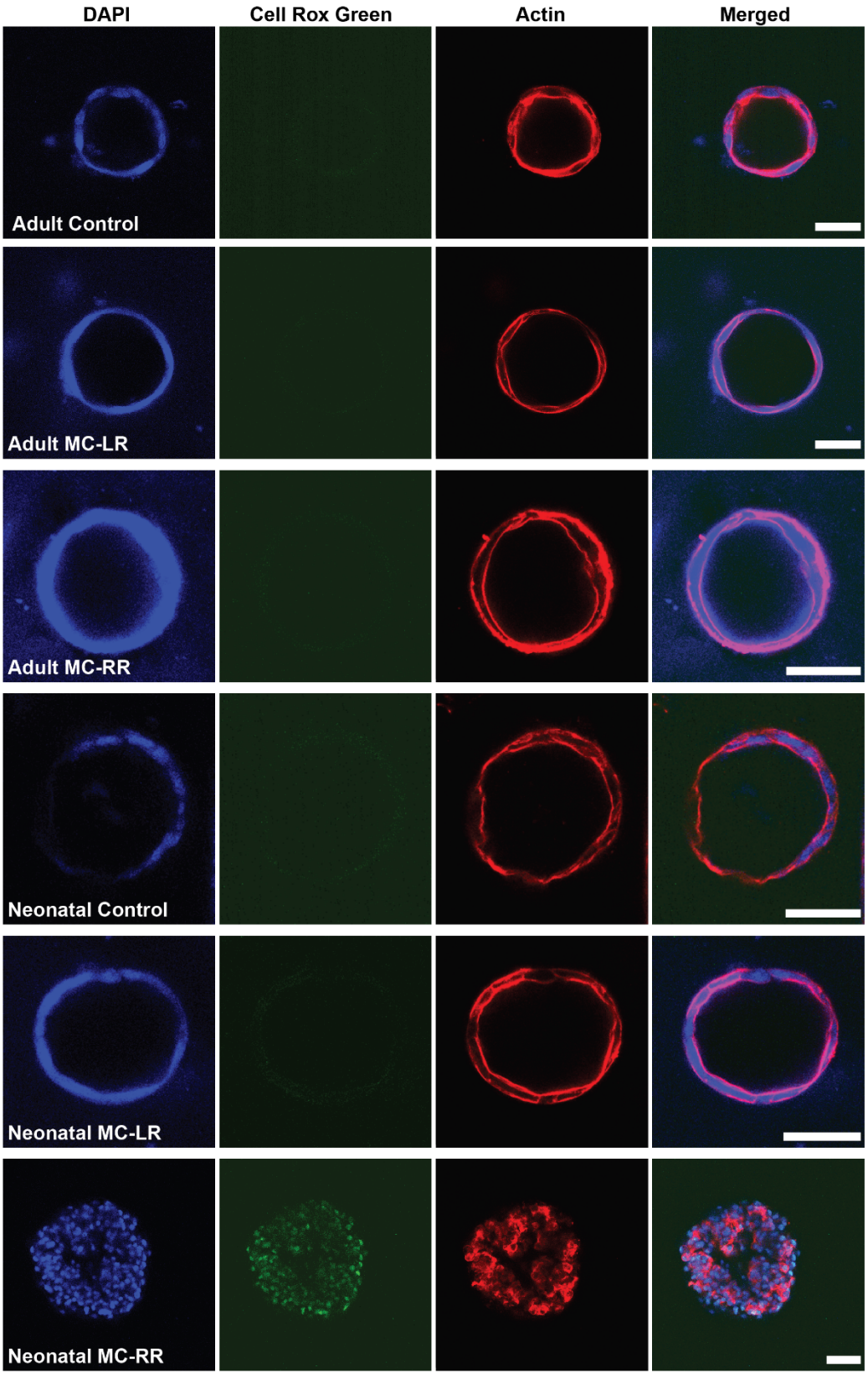

Supporting figure S10

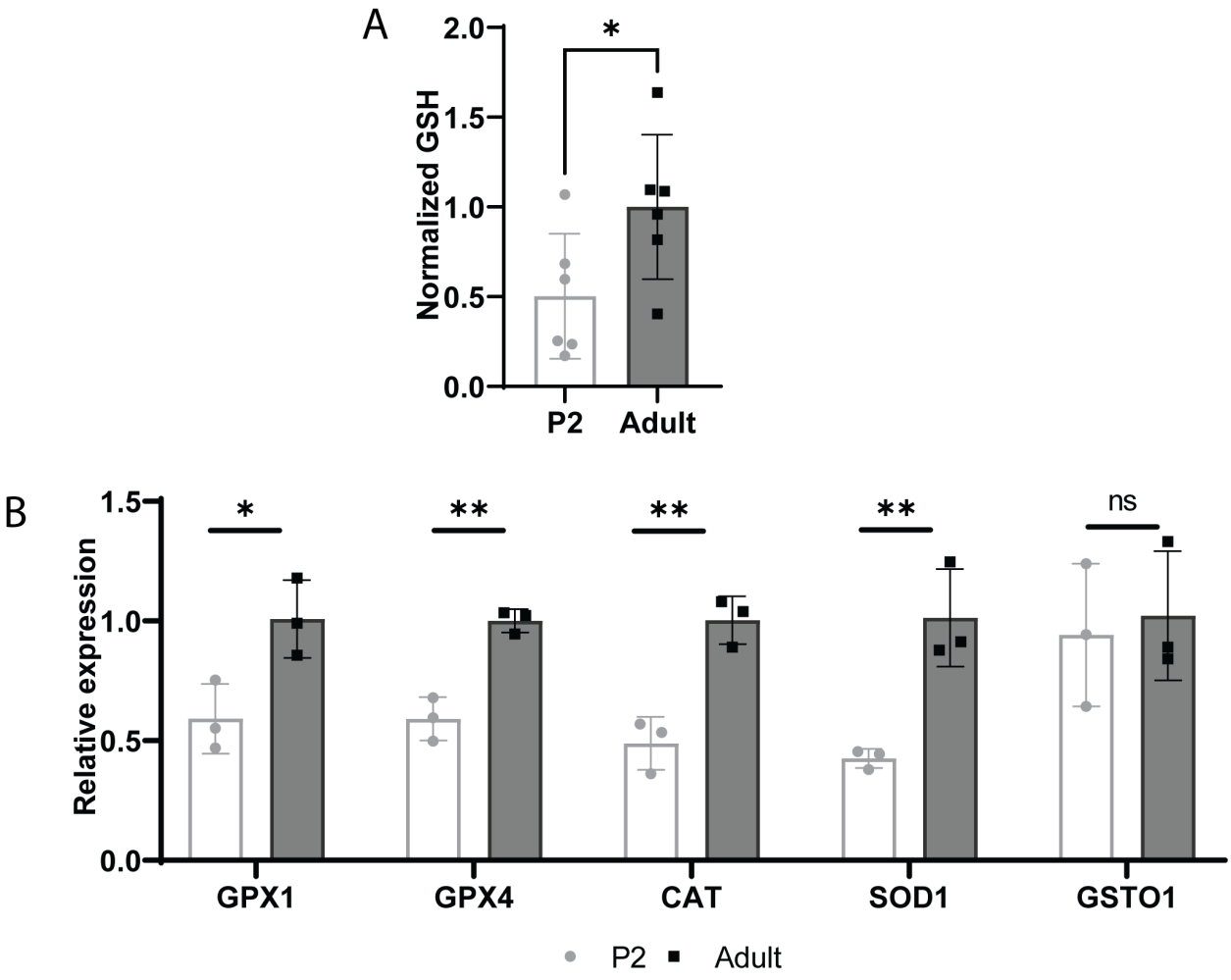

Supporting figure S11

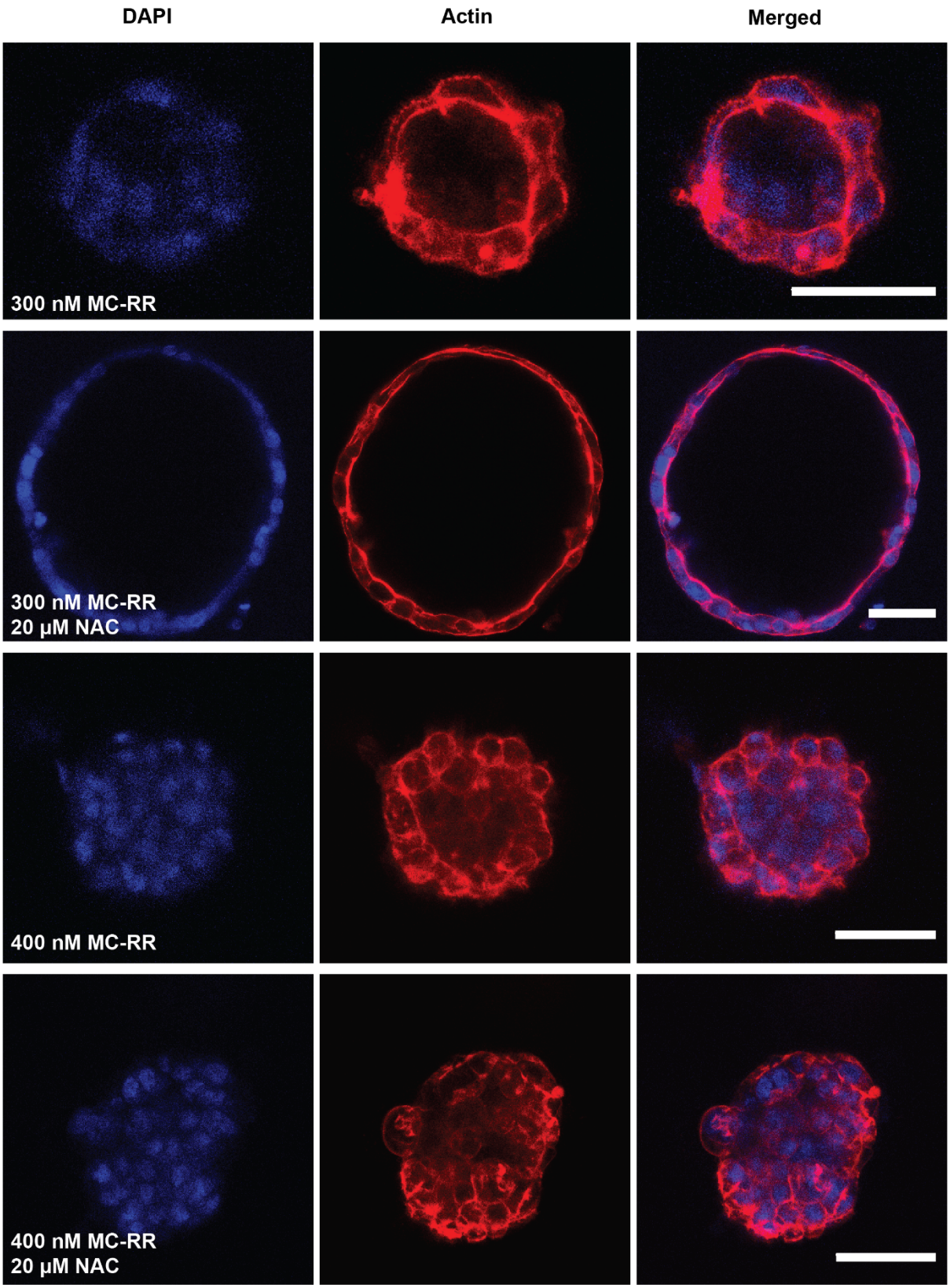

Supporting figure S12